

# Relativistic effects in polarizational bremsstrahlung.

A. V. Korol<sup>a</sup>, A. V. Solov'yov<sup>b</sup> ‡

<sup>a</sup> Department of Physics, Russian Maritime Technical University, Leninskii prospect 101, St. Petersburg 198262, Russia

<sup>b</sup> Frankfurt Institut for Advanced Studies, Johann Wolfgang Goethe-Universität, 60054 Frankfurt am Main, Germany

**Abstract.** We review the achievements of the theory of polarization bremsstrahlung of relativistic particles, including the case when both colliders have internal structure. The main features which the relativistic effects bring into the problem are discussed and illustrated by the results of numerical calculations.

## 1. Introduction.

In this paper we review the results of theoretical studies of the polarizational bremsstrahlung (PBrS) of relativistic atomic particles. Another review article from this issue [1] is devoted to the discussion of the PBrS process during various non-relativistic collisions. There a comprehensive historical review is given, and most of the terminology which is used to describe the PBrS process is introduced. Therefore, wherever possible we refer to [1] in order to avoid the repetition.

In what follows we focus on the specific features of PBrS (see figure 1b in [1]) which are due to the relativistic effects. The latter can be subdivided into the following categories. Firstly, there are effects directly related to the relativistic velocities of the particles involved in the process: *the velocity of a projectile* and/or *the velocity of the orbital motion* of electrons inside the colliders. To account for these effects one has to describe the dynamics of the colliders using the Dirac equation rather than the Schrödinger equation.

The relativistic effect of *retardation*, which modifies the interaction between a projectile and a target, we attribute to another category. Retardation implies that the relativistic particle polarizes the target not only through the Coulomb field, but also via the field of the transverse virtual photons (e.g. [2]), or, in terms of classical electrodynamics, via the retarded vector potential [3]. The effective radius of this field increases infinitely as the velocity  $v_1$  of the projectile approaches the velocity of light  $c$ . Therefore, the ultra-relativistic charge,  $v_1 \approx c$ , polarizes the target mainly via the exchange of the transverse virtual photons.

‡ On leave from: Ioffe Physical-Technical Institute, Russian Academy of Sciences, St. Petersburg 194021, Russia

There are relativistic effects due to the *multipole character* of radiation emitted by the target electrons. The multipolarity of the PBrS radiation depends solely on the magnitude of  $kR_{\text{at}}$ , where  $k$  is the photon momentum and  $R_{\text{at}}$  is the (mean) radius of the orbit of the electron who radiates. If this parameter is small, then the dipole-photon approximation is applicable, if otherwise, then it is necessary to take into account the radiation in higher multipoles.

Finally, in the case when both colliders are complex particles (for example, atom-atom, atom-ion, ion-ion pairs) it is necessary to account for the relativistic Doppler effect and the aberration of radiation. These are important factors which modify the PBrS of a relativistic complex projectile.

The role of the relativistic effects mentioned above was studied in [4–14] in various collisions of isolated atomic particles. In this paper we review the results obtained in the cited papers.

The influence of a dense medium on the features of PBrS of relativistic electrons was investigated in [15–19]. This issue is beyond the scope of our review and is not discussed below. We do not discuss the properties of the ordinary BrS of relativistic particles. The list of corresponding references (although not the fullest one) can be found [1, 12]. Finally, the main topic of this review concerns the relativistic effects in the PBrS process, therefore, we omitted the description of general features of PBrS in the non-relativistic domain as well as the historical survey. These could be found in [1, 20].

In the first two papers on relativistic PBrS formed in a collision of a charged structureless particle with an isolated atom (ion) [4, 5] the process was treated within the framework of the relativistic plane-wave Born approximation for the projectile and in the non-relativistic approximation for the target electrons. The retardation effect was accounted for, whereas the emission of the photon via the polarizational mechanism was considered in the dipole-photon approximation. The following two important features were established in these papers. Firstly, it was demonstrated that the PBrS cross section increases logarithmically with the energy  $\varepsilon_1$  of a projectile. This feature is a result of the retardation in the projectile–atom interaction. Secondly, it was shown that the shape of the angular distribution of PBrS, in contrast to the ordinary BrS, is proportional to  $(1 + a \cos^2 \theta)$  ( $\theta$  is the emission angle) where the coefficient  $a$  weakly depends on  $\varepsilon_1$ . This feature reflects the nature of the PBrS process in which the radiation occurs due to the alteration of the induced dipole moment of the target during the collision. We discuss these features in more detail in section 2.

Also, it was demonstrated [4] that the amplitude  $f_{\text{pol}}$  of the dipole PBrS can be expressed in terms of two polarizabilities, which define the dynamic atomic response to the joint actions of the fields of the projectile and of the dipole photon. In addition to the polarizability  $\alpha(\omega, q)$ , which accounts for the (non-retarded) Coulomb interaction between the projectile and the target, and which defines the PBrS of a non-relativistic projectile (see Eq. (1) in [1]), there is another polarizability,  $\beta(\omega, q)$ , which describes the dynamic response to the retarded vector potential created by the projectile. In the

limit  $q \ll R_{\text{at}}^{-1}$  both polarizabilities are expressed via the dynamic dipole polarizability  $\alpha_{\text{d}}(\omega)$  of the target. Small values of the transferred momenta  $q$  correspond to large distances between the projectile and the target,  $r \gg R_{\text{at}}$ , which are important for the PBrS mechanism [21, 22]. This fact, known from the non-relativistic theory of PBrS, was utilized in [4, 5] to derive the formulae for the PBrS spectrum and angular distribution within the large-distance approximation (another term is ‘the logarithmic approximation’ [21, 22]). In [10] the ‘logarithmic’ approximation was applied to study the total BrS process (i.e. the polarizational and the ordinary channels) in combination with the use of the local density method for the computation of  $\alpha_{\text{d}}(\omega)$ .

In [9] an approach was suggested for calculating the total BrS spectrum in relativistic electron-atom scattering utilizing a relativistic modified Elwert-Born approximation for the ordinary component of the spectrum but considering the PBrS within the non-relativistic ‘stripping’ approximation [23, 24].

The theory of PBrS formed in a collision of a charged particle with a many-electron atom/ion was developed further in the papers [11–14] where the fully relativistic formalism and the results of numerical calculations were presented. The formalism developed in these papers accounts for the relativistic effects of all types mentioned above (with the exception for the Doppler shift and aberration which are irrelevant in the case of a structureless projectile). The approach was based on the use of the distorted partial wave formalism for the description of the scattering process. The states of the target’s electrons were described in terms of single-electron relativistic wavefunctions. The effect of retardation and the multipole expansion of the emitted photon wave were accounted for. It was demonstrated that the full relativistic PBrS amplitude is expressed in terms of the multipole generalized target polarizabilities of three different types corresponding to the allowed combinations of the types of virtual and emitted photons coupled in the amplitude. On the basis of the relativistic formulae for the amplitude and the cross section obtained in [12, 13] the results, which had been obtained within the frameworks of the various simpler approaches, were evaluated by considering the corresponding limiting procedures. It was shown that the relativistic effects lead to noticeable changes in the spectral and angular characteristics of PBrS. A more detailed discussion is presented in section 2.

The PBrS mechanism defines the emission spectrum in collision of two complex particles, such as atoms or ions. The relativistic theory of such processes was developed in [6–8] where the details of the formalism were presented and the analysis of a number of physical phenomena and limiting cases was carried out. The important difference between the radiation formed in the atom–atom (or ion–ion/atom) collision from the collision of a structureless particle with an atom/ion is that in the former case both colliders emit photons via the polarization mechanism (the ordinary BrS of the projectile is negligibly small because of the large mass). The PBrS of the target, which is at rest in a laboratory frame, bears the same features as in the particle-atom/ion collision. On the contrary, the spectrum and the angular distribution of PBrS emitted by a relativistic complex projectile is strongly influenced by the relativistic Doppler shift

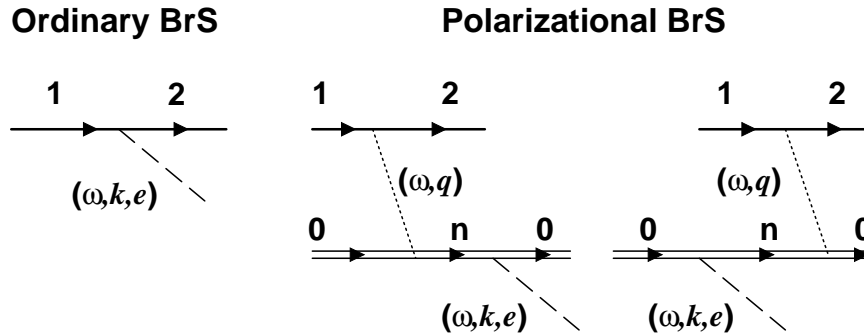


**Figure 1.** Diagrammatical representation of the BrS process (ordinary and polarizational) for a relativistic structureless charged projectile scattered by a many-electron atom. The solid lines correspond to the relativistic projectile which moves in a central field of the target. The initial ('1') and the final ('2') states of the projectile are characterized by the asymptotic momenta  $\mathbf{p}_{1,2}$  and the polarizations  $\mu_{1,2}$ . The double lines denote the states of the target: index '0' marks the initial and the final states, index 'n' corresponds to the intermediate virtual state. The dashed lines designate the emitted (real) photon of energy  $\omega$ , momentum  $\mathbf{k}$  and the polarizational vector  $\mathbf{e}$ . The dotted lines stand for the virtual photon, the energy of which is also  $\omega$  but the momentum  $\mathbf{q}$  is not fixed by any kinematic relations.

and the aberration of radiation. This influence manifests itself differently, depending on the magnitude of the photon energy  $\omega$  measured in the rest frame of the projectile. For high values of  $\omega$  the radiation, measured in the laboratory frame, is concentrated in the cone  $\theta \sim \gamma^{-1}$  ( $\gamma$  is the relativistic Lorentz factor of the projectile). For small values of  $\omega$  the angular distribution is nearly isotropic. Therefore, as it was pointed out in [7,8] for sufficiently high velocities of the collision there is a principal possibility to separate the radiation from the two colliders. Another important feature of the BrS process at relativistic velocities, which is also due to the Doppler and the aberration effects, is that the intensity of the dipole radiation formed in symmetric collisions does not vanish. In some more detail these and some other effects are discussed in section 3.

## 2. Polarizational BrS in collisions of structureless particles with atoms.

The BrS process in the collision between a relativistic projectile of charge  $Z_p e$  and mass  $m$  and a target atom is the transition of the projectile from the initial state  $(\mathbf{p}_1, \mu_1)$  to the final state  $(\mathbf{p}_2, \mu_2)$  accompanied by the emission of the photon. The energies of the particle in the initial and the final states are found from  $\varepsilon_{1,2} = (p_{1,2}^2 + m^2)^{1/2}$  (in this section we use the relativistic system of units  $\hbar = m_e = c = 1$ ). This radiative transition can occur via two mechanisms, as it is illustrated by the Feynman diagrams presented in figure 1. The first diagram describes the ordinary BrS amplitude,  $f_{\text{ord}}$ . The two other diagrams represent the polarizational part of the amplitude,  $f_{\text{pol}}$ .

The relativistic formalism of the derivation of the OBrS amplitude within the first Born approximation, or a more sophisticated one, based on the use of Sommerfeld-Maue

functions, can be found in textbooks (e.g. [2, 25]). The description in the framework of the distorted partial-wave approximation (DPWA) is also available [26, 27].

In what follows we outline the principal steps of the evaluation of the PBrS amplitude  $f_{\text{pol}}$  focusing on the differences between the full relativistic description from the non-relativistic one. For the sake of clarity we assume that the spin of a projectile is equal to 1/2, and, therefore, its bi-spinor wavefunction satisfies the Dirac equation which accounts for the central field of the target. It is a not severe restriction, and all the formulae can be easily re-written for the relativistic projectiles of other value of the spin.

As in the non-relativistic case, the photon emission via the polarizational mechanism occurs due to the virtual excitations of the target electrons under the action of two fields: the field created by the charged projectile (i.e. the field of the virtual photon) and the field of the emitted (real) photon.

With the effect of retardation accounted for, the field of the virtual photon is characterized by the 4-potential,  $A_\nu$  ( $\nu = 0, 1, 2, 3$ ), whose components are given by

$$A_\nu = Z_p e \sum_{a=1}^N \int d\mathbf{r} \Psi_{\mathbf{p}_2 \mu_2}^{(-)\dagger}(\mathbf{r}) \gamma^\mu D_{\mu\nu}(\omega, \mathbf{r} - \mathbf{r}_a) \Psi_{\mathbf{p}_1 \mu_1}^{(+)}(\mathbf{r}). \quad (1)$$

Here  $\Psi_\nu^{(\pm)}(\mathbf{r})$  are the bi-spinor wavefunctions corresponding to the out- (the upper index '+') and to the in- ('-') scattering states of the projectile, the symbol  $\dagger$  denotes the hermitian conjugation,  $\gamma^\mu$  ( $\mu = 0, 1, 2, 3$ ) are the Dirac matrices. The quantity  $D_{\mu\nu}(\omega, \mathbf{r} - \mathbf{r}_a)$  stands for the photon propagator. The sum is carried out over the target electrons,  $\mathbf{r}_a$  is the coordinate of the  $a$ th electron.

The scalar part of the 4-vector (1)  $A_0 \equiv \Phi$  defines the non-retarded Coulomb part of the interaction, the spatial components of  $A_\nu$  ( $\nu = 1, 2, 3$ ) define the retarded vector potential  $\mathbf{A}$  created by the projectile.

The consistent treatment of the relativistic effects in the PBrS process implies that it is necessary to retain all multipoles when describing the the vector potential  $\mathbf{A}_\gamma$  of the emitted real photon:

$$\mathbf{A}_\gamma = \sum_{a=1}^N \mathbf{e} e^{-i\mathbf{k}\mathbf{r}_a}. \quad (2)$$

Within the framework of perturbation theory the amplitude of PBrS is given by the sum of two second-order matrix elements which correspond to the atom's transition  $0 \rightarrow n \rightarrow 0$  under the action of the fields  $\mathbf{A}_\gamma$  and  $A_\nu$ :

$$f_{\text{pol}} = -e^2 \sum_n \left\{ \frac{\langle 0 | \boldsymbol{\gamma} \mathbf{A}_\gamma | n \rangle \langle n | \gamma^\nu A_\nu | 0 \rangle}{\varepsilon_n(1 - i0) - \varepsilon_0 - \omega} + \frac{\langle 0 | \gamma^\nu A_\nu | n \rangle \langle n | \boldsymbol{\gamma} \mathbf{A}_\gamma | 0 \rangle}{\varepsilon_n(1 - i0) - \varepsilon_0 + \omega} \right\} \quad (3)$$

The sum is carried out over the quantum numbers of the complete spectrum of the (virtual) excited atomic states and contains the contributions of the positive-energy,  $\varepsilon_n > 0$ , and the negative-energy,  $\varepsilon_n < 0$ , states.

The structure of the right-hand side of (3) is similar to the non-relativistic case (see Eq. (13) in [1]). The difference is that in (3) all the quantities which refer to the particles are treated relativistically.

### 2.1. The limiting cases of the amplitude (3).

Let us demonstrate how the expressions for  $f_{\text{pol}}$ , which one can derive within the frameworks of simpler theories, follow from the general relativistic formula (3).

The *non-relativistic dipole-photon limit* of (3) one can obtain using the following transformations. Firstly, carrying out the non-relativistic limit with respect to the projectile, one notices that the vector potential  $\mathbf{A}$  (which is due to the interaction retardation) can be neglected because of the relation  $|\mathbf{A}|/|\Phi| \sim v_{1,2} \ll 1$ . Therefore, only the Coulomb component the 4-potential  $A_\nu$  survives, where one uses  $D_{00}(\omega, \mathbf{r} - \mathbf{r}_a) = 1/|\mathbf{r} - \mathbf{r}_a|$ . Secondly, carrying out the limit  $k \rightarrow 0$  in (2) one makes a substitution  $\gamma \mathbf{A}_\gamma \rightarrow \mathbf{e} \sum_{a=1}^N \hat{\mathbf{p}}_a \equiv \mathbf{e} \hat{\mathbf{P}}$  where  $\hat{\mathbf{P}}$  is the momentum operator of all atomic electrons. The third step is to substitute  $\gamma^\nu A_\nu$  with its non-relativistic analogue equal to  $Z_p e \sum_a \langle \mathbf{p}_2^{(-)} | 1/|\mathbf{r} - \mathbf{r}_a| | \mathbf{p}_1^{(+)} \rangle$ . As a result of these transformations the sum over the negative-energy continuum in (3) becomes identically equal to zero, whereas the positive-energy sum reduces to the non-relativistic limit of  $f_{\text{pol}}$  (see Eq. (13) in [1]).

To obtain the PBrS amplitude within the framework of *relativistic plane-wave first Born approximation* (RBA) one substitutes the initial and the final wavefunctions of the projectile with the field-free Dirac bi-spinors (see, e.g., [25])

$$\Psi_{\mathbf{p}\mu}^{(\pm)}(\mathbf{r}) = u_\mu(\varepsilon, \mathbf{p}) e^{i\mathbf{p}\mathbf{r}} \quad (4)$$

where  $u_\mu(\varepsilon, \mathbf{p})$  is the field-free bi-spinor amplitude, and arrives at the expression derived in [12, 13].

If, within the RBA, one carries out *the non-relativistic limit with respect to the target's states*, and, additionally, *the dipole-photon limit*  $k \rightarrow 0$ , the resulting formula reduces to the expression which was obtained for the first time in [4]:

$$f_{\text{pol}} = -4\pi \omega Z_p e \left[ b^0 \frac{\mathbf{e}\mathbf{q}}{q^2} \alpha(\omega, q) - \frac{\mathbf{e}\mathbf{R}}{\omega^2 - q^2} \beta(\omega, q) \right]. \quad (5)$$

Here  $\mathbf{q} = \mathbf{p}_1 - \mathbf{p}_2$  is the momentum transfer,  $\mathbf{R} = \mathbf{b} - \mathbf{q}(\mathbf{b}\mathbf{q})/q^2$  and the quantities  $b^0$  and  $\mathbf{b}$  constitute a four-vector  $b^\mu = \bar{u}_{\mu_2}(\varepsilon_2, \mathbf{p}_2) \gamma^\nu u_{\mu_1}(\varepsilon_1, \mathbf{p}_1)$ . The first term in the brackets contains the non-relativistic generalized polarizability  $\alpha(\omega, q)$  of the target. This quantity enters the formula for the non-relativistic PBrS amplitude, where it defines the dynamic response of the target to the action of two fields: the Coulomb field of the projectile and the field of the dipole photon (see [1], Eq. (1)). The second term in the brackets is due to the retardation of the interaction between the projectile and the target. It is proportional to another non-relativistic polarizability,  $\beta(\omega, q)$ , which is responsible for the dynamic response of the target to the action of the retarded vector potential  $\mathbf{A}$  and the dipole-photon field. Explicit expressions for  $\alpha(\omega, q)$  and  $\beta(\omega, q)$  can be found in [4, 12, 13].

From formula (5) one easily derives the PBrS amplitude written within the frameworks of the *non-relativistic Born approximation and the dipole-photon approximation*. Carrying out the limit  $v_{1,2} \rightarrow 0$  one obtains  $b^0 = 1$  and  $\mathbf{b} = \mathbf{0}$ . This results in  $f_{\text{pol}} = -4\pi Z_p e(\mathbf{e}\mathbf{q}) \omega \alpha(\omega, q)/q^2$ , which is a well-known result in the non-relativistic theory of PBrS.

Finally, let us briefly discuss the *high-energy photon limit* of the PBrS amplitude, i.e. when the photon energy exceeds the magnitude of the  $K$ -shell ionization potential  $\omega \gg I_{1s}$  [12]. In the non-relativistic dipole-photon theory this limit is called the ‘stripping’ approximation [23, 24]. In [12] this limit was considered within the framework of the following approximation: relativistic description of the projectile but non-relativistic treatment of the target. The effects of the retardation and the emission into higher multipoles are taken into account.

Similar to the non-relativistic dipole-photon case [28] the PBrS amplitude can be represented as a matrix element of the effective operator  $V_{\text{eff}}$  calculated between the scattering states of the projectile. Omitting the details we present the final result for  $f_{\text{pol}}$  in this limit:

$$f_{\text{pol}} = \langle \mathbf{p}_2 \mu_2 | V_{\text{eff}}(\mathbf{r}) | \mathbf{p}_1 \mu_1 \rangle \quad (6)$$

where the operator of  $V_{\text{eff}}(\mathbf{r})$  is given by

$$V_{\text{eff}}(\mathbf{r}) = i \frac{e^2}{m\omega^2} \int d\mathbf{r}' \rho(r') e^{-i\mathbf{k}\mathbf{r}'} \left[ \gamma_0 \frac{\mathbf{e}(\mathbf{r} - \mathbf{r}')}{|\mathbf{r} - \mathbf{r}'|} \left( k + \frac{i}{|\mathbf{r} - \mathbf{r}'|} \right) + k \mathbf{e}\boldsymbol{\gamma} \right] \frac{e^{ik|\mathbf{r}-\mathbf{r}'|}}{|\mathbf{r} - \mathbf{r}'|}. \quad (7)$$

Here  $\rho(r')$  is the density of the electron cloud of the target atom.

These formulae generalize the result of the non-relativistic dipole photon treatment of the PBrS process within the frame of the ‘stripping’ approximation [28, 29]. Indeed, carrying out the limit  $k = 0$  in (7) and substituting in (6) the relativistic wavefunctions with the non-relativistic ones one obtains  $f_{\text{pol}} = -\omega^{-2} \langle \mathbf{p}_2 | \mathbf{e}\mathbf{a}_{el} | \mathbf{p}_1 \rangle$  where  $\mathbf{a}_{el}$  is the acceleration of the projectile due to the static field created by the atomic electrons (see Eq. (22) in [1]).

## 2.2. The relativistic DPWA and multipole series for $f_{\text{pol}}$ .

To derive the partial-wave series and the multipole series of the amplitude (3) one can use the following procedure [12]. To start with one uses the relativistic DPWA series for the wavefunctions  $\Psi_{\mathbf{p}\mu}^{(\pm)}(\mathbf{r})$  (see, e.g., [2]):

$$\Psi_{\mathbf{p}\mu}^{(\pm)}(\mathbf{r}) = \frac{4\pi}{pr} \sum_{jlm} \left( \Omega_{jlm}^\dagger(\mathbf{n}_{\mathbf{p}}) \chi_\mu(\mathbf{n}_{\mathbf{p}}) \right) e^{\pm i\delta_{jl}(\varepsilon)} \begin{pmatrix} g(r) \Omega_{jlm}(\mathbf{n}_{\mathbf{r}}) \\ -if(r) (\boldsymbol{\sigma}\mathbf{n}_{\mathbf{r}}) \Omega_{jlm}(\mathbf{n}_{\mathbf{r}}) \end{pmatrix}. \quad (8)$$

Here a general notation  $\mathbf{n}_{\mathbf{a}}$  is used for the unit vector in the direction of  $\mathbf{a}$ ,  $\Omega_{jlm}(\mathbf{n}_{\mathbf{p}})$  and  $\Omega_{jlm}(\mathbf{n}_{\mathbf{r}})$  are the spherical spinors defined as in [30],  $\chi_\mu$  stands for a two-component spinor corresponding to the spin projection  $\mu$ , the quantities  $\delta_{jl}(\varepsilon)$  are the scattering phaseshifts,  $\boldsymbol{\sigma}$  is the Pauli matrix. The functions  $g(r) \equiv g_{\varepsilon jl}(r)$  and  $f(r) \equiv f_{\varepsilon jl}(r)$  are, correspondingly, the large and the small components of the relativistic radial

wavefunction in the central field of the target. The sum is carried out over the total momentum  $j$ , orbital momentum  $l$  and the projection  $m$  of the total momentum.

The next step is to introduce the multipole expansions of the factors  $\mathbf{e}\boldsymbol{\gamma} \exp(-i\mathbf{k}\mathbf{r})$  and  $\exp(-i\mathbf{q}\mathbf{r})$  (the latter appears in  $A_\nu$  from (1)) in terms of the vector spherical harmonics  $\mathbf{Y}_{lm}^{(\lambda)}(\mathbf{n})$  ( $\lambda = 0, 1$ ) and the spherical harmonics  $Y_{lm}(\mathbf{n}) = \mathbf{n}\mathbf{Y}_{lm}^{(-1)}(\mathbf{n})$  [30].

Finally, assuming that the states  $|0\rangle$  and  $|n\rangle$  of the target can be described in terms of single-electron wavefunctions (see, e.g., [31]), one converts the sums over the atomic states  $n$  from (3) into the sums over the quantum numbers,  $\varepsilon_i, j_i, l_i, m_i$  ( $i = 0, n$ ) of the core and the excited subshells. The bi-spinor single-electron wavefunctions,  $\Psi_{\varepsilon_i j_i l_i m_i}(\mathbf{r})$ , can be obtained by solving the system of self-consistent radial Hartree-Fock-Dirac equations (see, e.g., [32]).

Having done all this and carrying out the intermediate algebra, one obtains the following expression for  $f_{\text{pol}}$  written in terms of the multipole series over  $\mathbf{Y}_{lm}^{(\lambda)}(\mathbf{n}_{\mathbf{k}})$  and the DPWA series with respect to the initial and the final states of the projectile:

$$f_{\text{pol}} = i \frac{(4\pi)^{5/2} Z_p e}{p_1 p_2} \sum_{\substack{j_1 l_1 m_1 \\ j_2 l_2 m_2}} \sum_{\substack{\lambda=0,1 \\ lm}} (-1)^{m_1 + \frac{1}{2}} i^{-l-\lambda} e^{i\delta_{j_1 l_1}(\varepsilon_1) + i\delta_{j_2 l_2}(\varepsilon_2)} (\chi_{\mu_2}^\dagger \Omega_{j_2 l_2 m_2}) \left( \Omega_{j_1 l_1 m_1}^\dagger \chi_{\mu_1} \right) \\ \times \xi(l_2 l_1 l \lambda 1) \Pi_{j_1 j_2 l} \begin{pmatrix} j_2 & j_1 & l \\ -m_2 & m_1 & -m \end{pmatrix} \begin{pmatrix} j_2 & j_1 & l \\ \frac{1}{2} & -\frac{1}{2} & 0 \end{pmatrix} \mathbf{e}\mathbf{Y}_{lm}^{(\lambda)}(\mathbf{n}_{\mathbf{k}}) \mathcal{P}_{21}^{(\lambda)}(\omega, k, l), \quad (9)$$

where  $\begin{pmatrix} a & b & c \\ \alpha & \beta & \gamma \end{pmatrix}$  stands for the  $3j$ -symbol, and the short-hand notation  $\Pi_{j_1 j_2 \dots} = \sqrt{(2j_1 + 1)(2j_2 + 1) \dots}$  is used [30]. The function  $\xi(l_2 l_1 l \lambda 1)$  equals to one if the sum of its arguments is even, and equals to zero if otherwise.

The quantities  $\mathcal{P}_{21}^{(\lambda)}(\omega, k, l)$  ( $\lambda = 0, 1$ ) are the relativistic partial amplitudes of the PBrS. They depend, apart from the quantum numbers  $\omega, k, l$  on the combination of the types of the real and the virtual photons entangled in the amplitude. For a spherically-symmetric target there are three allowed combinations of virtual and real photons: longitudinal-electric, electric-electric and magnetic-magnetic. The first two combinations are incorporated in the amplitude  $\mathcal{P}_{21}^{(1)}(\omega, k, l)$  which consists of two terms,  $\mathcal{P}_{21}^{(l)}(\omega, k, l) + \mathcal{P}_{21}^{(e)}(\omega, k, l)$ . The partial amplitude  $\mathcal{P}_{21}^{(0)}(\omega, k, l)$  corresponds to the magnetic-magnetic combination. The explicit expressions for these terms are as follows:

$$\mathcal{P}_{21}^{(l)}(\omega, k, l) = -\frac{2}{\pi} \frac{\sqrt{l(l+1)}}{2l+1} \int_0^\infty q dq \alpha_l(\omega, q, k) f_{21}^{(-1)}(q; l) \quad (10)$$

$$\mathcal{P}_{21}^{(e)}(\omega, k, l) = \frac{2}{\pi} \frac{[l(l+1)]^{3/2}}{2l+1} \int_0^\infty \frac{q^2 dq}{k^2 - q^2 + i0} \beta_l^{(1)}(\omega, q, k) f_{21}^{(1)}(q; l) \quad (11)$$

$$\mathcal{P}_{21}^{(0)}(\omega, k, l) = -\frac{2}{\pi} \frac{\sqrt{l(l+1)}}{2l+1} \int_0^\infty \frac{q^2 dq}{k^2 - q^2 + i0} \beta_l^{(0)}(\omega, q, k) f_{21}^{(0)}(q; l). \quad (12)$$

Here  $f_{21}^{(-1,0,1)}(q; l)$  stand for the radial integrals which contain the radial wavefunctions (the large and small components) of the initial and the final states of the projectile and the spherical Bessel functions  $j_l(qr)$ . The corresponding formulae can be found in [12].



The most important feature of the formulae (10)–(12) is that they clearly demonstrate that in the relativistic case the PBrS amplitude is expressed in terms of the multipole generalized dynamic polarizabilities of three different types corresponding to the allowed combinations of the types of the virtual/real photons: (a)  $\alpha_l(\omega, q, k)$  corresponds to the longitudinal/electric combination, (b)  $\beta_l^{(1)}(\omega, q, k)$  to the electric/electric one, and (c)  $\beta_l^{(0)}(\omega, q, k)$  to the magnetic/magnetic. Each of these polarizabilities depends on the photon energy  $\omega$ , its orbital momentum  $l$  (which defines the multipolarity of the polarizability), and on the magnitudes of the momenta  $q$  and  $k$  of the virtual and real photons. We do not reproduce here the explicit expressions for the polarizabilities but refer to the papers [12, 13] where various representations are given and discussed in detail.

In the non-relativistic limit (with respect to both the projectile and to the target) and in the *dipole-photon* approximation ( $k = 0$ ) the amplitudes  $\mathcal{P}_{21}^{(e)}(\omega, k, l)$  and  $\mathcal{P}_{21}^{(0)}(\omega, k, l)$  vanish for all  $l$ . The only term which survives is  $\mathcal{P}_{21}^{(l)}(\omega, k, l)$  with  $l = 1$ . The corresponding generalized polarizability  $\alpha_1(\omega, q, 0)$  reduces to the non-relativistic polarizability  $\alpha(\omega, q)$ , and the partial amplitude  $\mathcal{P}_{21}^{(1)}(\omega, 0, l)$  reproduces the non-relativistic expression (see Eq. (18) in [1]).

Let us note that the polarizability  $\beta(\omega, q)$  introduced above in Eq. (5) is equal to  $\beta_1^{(1)}(\omega, q, 0)$ .

Finally, we mention that the structure of the DPWA and multipole series for the OBrS amplitude is similar to that of the right-hand side of (9). Therefore, to obtain the total BrS amplitude,  $f_{\text{tot}} = f_{\text{ord}} + f_{\text{pol}}$  one substitutes  $\mathcal{P}_{21}^{(\lambda)}(\omega, k, l)$  in (9) with  $\mathcal{T}_{21}^{(\lambda)}(\omega, k, l) = \mathcal{P}_{21}^{(\lambda)}(\omega, k, l) + \mathcal{O}_{21}^{(\lambda)}(\omega, k, l)$ , where  $\mathcal{O}_{21}^{(\lambda)}(\omega, k, l)$  are the OBrS partial amplitudes [12]. In the non-relativistic limit, carried out with respect to the projectile motion and the states of atomic electrons, and in the dipole-photon limit the DPWA series (9) reproduce the formulae presented in [33].

### 2.3. The cross section of relativistic PBrS

The expansion (9) allows one to derive the DPWA and multipole series for the spectral and spectral-angular distributions of PBrS (and the total BrS as well). The details of the formalism and the final results are presented in [12].

Aiming to point out the qualitative differences, which are model-independent, between the relativistic case and the non-relativistic one we discuss the PBrS cross section in terms of the relativistic plane-wave Born approximation.

We start with the discussion of the spectral distribution of PBrS,  $d\sigma_{\text{pol}}/d\omega$ . The corresponding cross section  $d\sigma_{\text{pol}}(\omega) = \omega (d\sigma_{\text{pol}}/d\omega)$  is given by [13]:

$$\begin{aligned}
 d\sigma_{\text{pol}}(\omega) = & \alpha \frac{2Z_p^2 \omega^2}{p_1^2} \sum_{l=1}^{\infty} \frac{l(l+1)}{2l+1} \int_{q_{\min}}^{q_{\max}} \frac{dq}{q} \left[ \left( q_{\min}^2 q_{\max}^2 - q^2 k^2 \right) |\alpha_l(\omega, q, k)|^2 \right. \\
 & \left. + l(l+1) \frac{2q^2(q^2 - k^2) + (q^2 - q_{\min}^2)(q_{\max}^2 - q^2)}{2(q^2 - k^2)^2} \sum_{\lambda=0,1} \left| \beta_l^{(\lambda)}(\omega, q, k) \right|^2 \right] \quad (13)
 \end{aligned}$$

Here  $\alpha$  is the fine structure constant,  $q = |\mathbf{p}_1 - \mathbf{p}_2|$  is the momentum transfer. Its minimum and maximum values are  $q_{\min} = p_1 - p_2$  and  $q_{\max} = p_1 + p_2$ .

The first term in the integrand, proportional to  $|\alpha_l(\omega, q, k)|^2$ , is due to the dynamic polarization of the target by the Coulombic part of the field of the projectile, whereas the second term, containing the polarizabilities  $\beta_l^{(\lambda)}(\omega, q, k)$  appears as the result of the retardation of the interaction. In the non-relativistic limit (with respect to the projectile and the target) and in the dipole-photon regime all polarizabilities but  $\alpha_1(\omega, q, k)$  are equal to zero. In this limit  $\alpha_1(\omega, q, k) \rightarrow \alpha(\omega, q)$ , which is the non-relativistic dipole generalized polarizability, and the right-hand side of (13) reduces to the non-relativistic PBrS cross section (see Eq. (24) in [1]). Similar to the non-relativistic result the cross section (13) weakly depends on the mass of a projectile.

An important distinguishing feature of the *relativistic* PBrS cross section is its logarithmic growth with  $\varepsilon_1$  [4, 5]. Qualitatively, the reason for this is as follows. As was already mentioned, unlike a non-relativistic particle, a relativistic one interacts with the target not only by its Coulomb field but also (in the ultra-relativistic case, predominantly) by the field of transverse virtual photons. The effective radius of this field,  $R_{\text{eff}}$ , increases infinitely with the energy of the projectile. The magnitude of  $R_{\text{eff}}$  can be estimated as  $R_{\text{eff}} \sim 1/q_{\min}^\perp$ , where  $q_{\min}^\perp \approx \gamma^{-1}q_{\min}$ , with  $\gamma = \varepsilon_1/m$  and  $q_{\min} = p_1 - p_2 \approx \omega/v_1$  [4]. As a result, the range of distances at which a projectile effectively polarizes a target increases. This leads to the growth of  $d\sigma_{\text{pol}}(\omega)$  with  $\varepsilon_1$ .

Quantitative description of this effect can be carried out directly from (13) by analyzing the contribution of the region  $q_{\text{at}} \geq q \geq q_{\min} \approx \omega/v_1$  to the integral (here  $q_{\text{at}} = R_{\text{at}}^{-1}$  with  $R_{\text{at}}$  being the radius of the target). The result reads [13]:

$$\left[ d\sigma_{\text{pol}}(\omega) \right]_{q \sim q_{\min}} \approx \alpha \frac{4Z_p^2 \omega^4}{v_1^2} \left( A \ln \frac{q_{\text{at}}}{q_{\min}} + B \ln \frac{\varepsilon_1}{m} \right) \quad (14)$$

where

$$A = \sum_{l=1}^{\infty} \frac{2l(l+1)}{2l+1} |\alpha_l(\omega, q_{\min}, k)|^2, \quad B = \frac{1}{\omega^4} \sum_{l=1}^{\infty} \frac{l^2(l+1)^2}{2l+1} \sum_{\lambda=0,1} \left| \beta_l^{(\lambda)}(\omega, q_{\min}, k) \right|^2. \quad (15)$$

The first term in term in the brackets on the right-hand side of (14) corresponds to the contribution of the Coulomb part of the interaction, and it remains constant as the energy  $\varepsilon_1$  grows. The second term, which is due to the interaction retardation, logarithmically increases with  $\varepsilon_1$ . This feature was first noted in [4, 5], where the PBrS of a relativistic projectile was studied within the framework of the non-relativistic dipole-photon description of the target. The result of these studies follows from more general expressions (14) and (15). Carrying out the non-relativistic dipole photon limit, and accounting for the relations  $\lim_{k \rightarrow 0} \alpha_1(\omega, q_{\min}, k) = \lim_{k \rightarrow 0} \omega^{-2} \beta_1^{(1)}(\omega, q_{\min}, k) \approx \alpha_d(\omega)$  if  $q_{\min} R_{\text{at}} \ll 1$  one obtains [4]:

$$d\sigma_{\text{pol}}(\omega) \approx \alpha \frac{16Z_p^2 \omega^4}{3v_1^2} \omega^4 |\alpha_d(\omega)|^2 \ln \frac{q_{\text{at}} \varepsilon_1}{mq_{\min}}, \quad (16)$$

where  $\alpha_d(\omega)$  is the dynamic (non-relativistic) dipole polarizability.

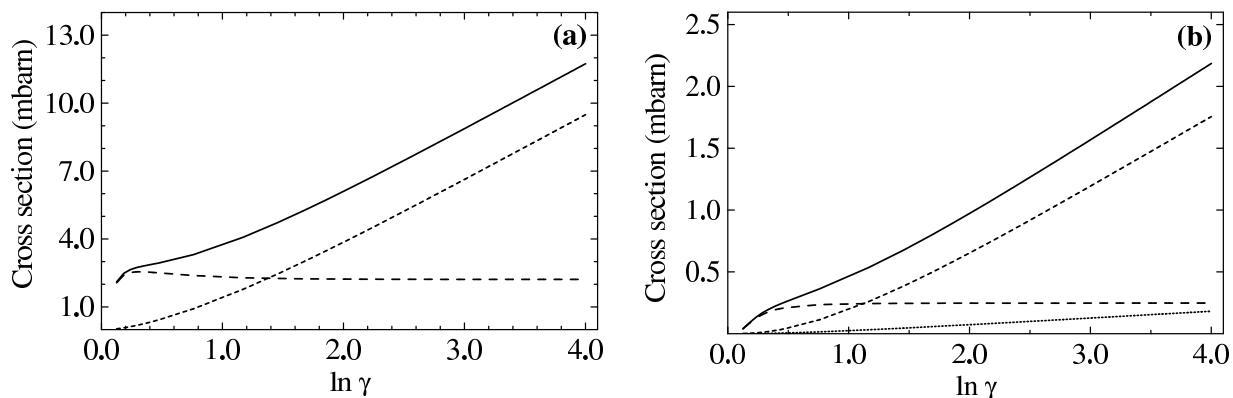


**Figure 2.** Dependence of  $d\sigma_{\text{pol}}(\omega)$  on  $\ln \gamma \equiv \ln(\varepsilon_1/m)$  for a proton- $\text{Au}^{+78}$  collision. Thick solid curve describes  $d\sigma_{\text{pol}}(\omega)$  with all terms on the right-hand side of (13) included. The long-dashed, the dotted and the short-dashed curves represent, respectively, the contributions of the terms containing the polarizabilities  $\alpha_l(\omega, q, k)$ ,  $\beta_l^{(0)}(\omega, q, k)$  and  $\beta_l^{(1)}(\omega, q, k)$ . In figure (a) the photon energy  $\omega$  equals to  $1.5I$ , in figure (b)  $\omega = 4I$  (where  $I = 93.5$  keV is the ionization potential of the target).

The logarithmic growth of  $d\sigma_{\text{pol}}(\omega)$  with  $\varepsilon_1$  is illustrated in figures 2a,b where the PBrS cross sections formed in the collision of a proton with a hydrogen-like gold are presented. Because of the large mass of the proton its OBrS is suppressed by the factor  $m^{-2} \sim 10^{-6}$ , and can be neglected. The data presented in the figures correspond to two values of  $\omega$  as indicated in the caption. The growth of the cross section, which is nearly linear for high values of  $\ln(\varepsilon_1/m)$  in accordance with (14) and (16), is due to the contribution of the terms containing  $\beta_l^{(0)}(\omega, q, k)$  and  $\beta_l^{(1)}(\omega, q, k)$  (see (13)). The contribution of the terms proportional to  $\alpha_l(\omega, q, k)$  is virtually independent on  $\varepsilon_1$ .

Expression (16) generalizes the result of non-relativistic theory. Indeed, putting  $\varepsilon_1 = m$  on the right-hand side one obtains the expression derived in [21,22], where it was called the ‘logarithmic approximation’ for PBrS. Let us note here that the OBrS cross section of a relativistic projectile in collision with a neutral target is almost independent on  $\varepsilon_1$  for high velocities of the projectile,  $v_1 \leq 1$ . Therefore, the total cross section also increases logarithmically with  $\varepsilon_1$ .

In the case of an ultra-relativistic electron or positron ( $m_e = Z_p^2 = 1$ ) scattering on a neutral target there is a peculiar feature of the total BrS cross section which is clearly distinct from the non-relativistic case. To demonstrate it we consider the limit of high energy photons when  $\omega \gg I_{1s}$ , and one can use the approximate formula for the dipole polarizability  $\alpha_d(\omega) \approx -Z/\omega^2$  ( $Z$  stands for the number of atomic electrons which for a neutral atom coincides with the atomic number). The PBrS cross section (16) reduces to  $d\sigma_{\text{pol}}(\omega) \approx 16\alpha/3 Z^2 \ln(q_{\text{at}}\varepsilon_1/\omega)$  where we used  $v_1 = 1$  and  $q_{\text{min}} = \omega$ . In the ‘logarithmic approximation’ the OBrS cross section is given by (see, e.g., [25])  $d\sigma_{\text{ord}}(\omega) \approx 16\alpha/3 Z^2 \ln(1/q_{\text{at}})$ . In the same approximation one can neglect the interference term and derive the following expression for the total BrS cross section:

$$d\sigma_{\text{tot}}(\omega) \approx d\sigma_{\text{ord}}(\omega) + d\sigma_{\text{pol}}(\omega) \approx Z^2 \frac{16\alpha}{3} \ln \frac{\varepsilon_1}{\omega}. \quad (17)$$

Apart from the factor  $Z^2$  the right-hand side of this equation reproduces the formula for the cross section of BrS emitted by a slow free electron in the collision with an ultra-relativistic electron or positron [25]. This coincidence is not accidental and has clear qualitative explanation [4]. For  $\omega \gg I_{1s}$  the atomic electrons can be treated as free ones. If  $Z\alpha \ll 1$  then the velocities of all atomic electrons are small compared to that of the projectile. Then, the total BrS amplitude can be written as the sum of three terms  $f_{\text{tot}} = Z\mathcal{F}_1 + Z\mathcal{F}_2 + \mathcal{F}_3$ . Here  $\mathcal{F}_1$  denotes the amplitude of the photon emission by the projectile electron/positron interacting with a free atomic electron,  $\mathcal{F}_2$  is the amplitude of the emission by the atomic electron during this interaction, and  $\mathcal{F}_3$  is the amplitude due to the interaction of the projectile with the nucleus. As known (see, e.g., [25]), the BrS amplitude of an ultra-relativistic electron/positron scattered from a free slow particle depends on the particle's charge and does not depend on its mass. Therefore, the sum of two terms,  $Z\mathcal{F}_1 + \mathcal{F}_3$  is identically equal to zero, and  $f_{\text{tot}}$  reduces to  $Z\mathcal{F}_1$ , i.e. only atomic electrons radiate in this process. In a way, this result is opposite to the 'stripping' effect in the non-relativistic BrS, when  $d\sigma_{\text{tot}}(\omega)$  in electron-atom collision reduces to that on the bare nucleus if  $\omega \gg I_{1s}$  (see Eq. (6) in [1]). The qualitative explanation of this difference between the non-relativistic and the ultra-relativistic cases is as follows. In the former case, the range of distances between the projectile and the target important in the PBrS process can be estimated as  $R_{\text{eff}} \sim 1/q_{\text{min}} \approx v_1/\omega$ . This value is much smaller than the photon wavelength  $\lambda = 2\pi/\omega$ . Therefore, the dipole approximation can be applied for the system 'the projectile + the target'. The only allowed radiation in this system in the range  $\omega \gg I_{1s}$  (the limit of quasi-free atomic electrons) is that by a projectile on the nucleus. As was already mentioned, in the ultra-relativistic case  $R_{\text{eff}} \sim 1/q_{\text{min}}^\perp \approx \gamma/\omega$ . As  $v_1 \rightarrow 1$  and  $\gamma \rightarrow \infty$  these distances increase unrestrictedly and are much greater than  $\lambda$ . The retardation effects in the interaction between the projectile and the atomic electron become important, so that the dipole approximation is inapplicable to this system. This leads to the difference of (17) from its non-relativistic analogue.

The retardation, as well as the relativistic and higher multipoles effects, strongly modify not only the PBrS spectral distribution but the spectral-angular distribution as well [13]. The spectral-angular distribution can be written in the form of series over the Legendre polynomials  $P_l(\cos \theta)$ :

$$d^2\sigma_{\text{pol}}(\omega, \Omega) \equiv \omega \frac{d^2\sigma_{\text{pol}}}{d\omega d\Omega} = \frac{d\sigma_{\text{pol}}(\omega)}{4\pi} \left( 1 + \sum_{l_k=1}^{\infty} a_{l_k}(\omega) P_{l_k}(\cos \theta) \right), \quad (18)$$

here  $\theta$  is the emission angle (measures with respect to  $\mathbf{p}_1$ ). The coefficients  $a_{l_k}(\omega)$  depend on the photon energy and are the bi-linear forms of the relativistic polarizabilities  $\alpha_l(\omega, q, k)$  and  $\beta_l^{(1,2)}(\omega, q, k)$ . The explicit formulae for  $a_{l_k}(\omega)$ , obtained within the DPWA and the relativistic Born approximation, can be found in the cited paper (see also [12]).

The expression for  $d^2\sigma_{\text{pol}}^{\text{NR}}(\omega, \Omega)$  obtained within the framework of non-relativistic

dipole-photon approximation reads [33, 34]:

$$d^2\sigma_{\text{pol}}^{\text{NR}}(\omega, \Omega) = \frac{d\sigma_{\text{pol}}^{\text{NR}}(\omega)}{4\pi} (1 + \beta(\omega) P_2(\cos\theta)) . \quad (19)$$

The quantity  $\beta(\omega)$  is frequently called a (dipole) coefficient of angular anisotropy.

Let us point to the differences between (18) and (19). The first one, already discussed above, concerns the different dependence of the factors  $d\sigma_{\text{pol}}(\omega)$  and  $d\sigma_{\text{pol}}^{\text{NR}}(\omega)$  on  $\varepsilon_1$ . The former increases proportionally to  $\ln(\varepsilon_1)$  and this is due to the retardation. The second difference, a rather obvious one, is reflected by an infinite number of terms on the right-hand side of (18), which are due to the infinite number of the photon multipoles taken into account, in contrast to the two terms in (19). Finally, there is a ‘hidden’ difference which is related to the relativistic description of the internal dynamics of the target rather than to the multipole character of the radiation. The easiest way to trace the origin of this difference is to consider the contribution of only dipole photons to the series in (18). The momentum of a dipole photon is  $l = 1$ , therefore only the amplitudes  $\mathcal{P}_{21}^{(l,e,m)}(\omega, k, 1)$  (see (10)–(12)) will contribute to the PBrS amplitude (9). Then, instead of (18) one obtains [13]:

$$\left[ d^2\sigma_{\text{pol}}(\omega, \Omega) \right]_{l=1} = \frac{\left[ d\sigma_{\text{pol}}(\omega) \right]_{l=1}}{4\pi} (1 + a_1(\omega) P_1(\cos\theta) + a_2(\omega) P_2(\cos\theta)) , \quad (20)$$

It is seen that in contrast to (19) the angular distribution of the relativistic *dipole* radiation contains the term proportional to  $P_1(\cos\theta)$ . As a result, the angular distribution becomes asymmetric with respect to the transformation  $\theta \rightarrow \pi - \theta$ .

The reason for this effect is as follows. If the target is treated within the non-relativistic framework then the dipole photons emitted via the polarizational mechanism belong to the ‘electric’ type [25]. This statement is valid for arbitrary velocities of the projectile. Indeed, for  $v_1 \ll 1$  the PBrS amplitude is proportional to  $\alpha(\omega, q)$  (see Eq. (1) in [1]) which couples the Coulomb field of a projectile and the field of the ‘electric’ dipole photon. For relativistic velocities,  $v_1 \leq 1$ , the amplitude  $f_{\text{pol}}$  contains two polarizabilities,  $\alpha(\omega, q)$  and  $\beta(\omega, q)$  (see (5)). The former couples the ‘electric’ dipole photon with the ‘electric’ dipole virtual photon. Due to the selection rules, the angular dependent part of the intensity of the ‘electric’ dipole radiation contains the term proportional to  $P_2(\cos\theta)$  only [25]. In the most explicit form this can be illustrated if one evaluates the angular distribution of PBrS using the ‘logarithmic approximation’. Then, either for a non-relativistic projectile [21] or a relativistic one [4] the PBrS angular distribution is proportional to  $1 + P_2(\cos\theta)/2 \propto 1 + \cos^2\theta$ , which coincides with the angular distribution of radiation emitted by a rotating electric dipole [3].

In the case when the internal dynamics of the target is treated within the relativistic theory, there appears a possibility to emit a photon of the ‘magnetic’ type. If the ‘magnetic’ dipole radiation is treated separately, its angular dependent part also contains the term proportional to  $P_2(\cos\theta)$  only [25]. However, if both types of the dipole photons can be emitted in a process, then their interference results in the term proportional to  $P_1(\cos\theta)$ . This is exactly what happens in the relativistic PBrS. Using the general

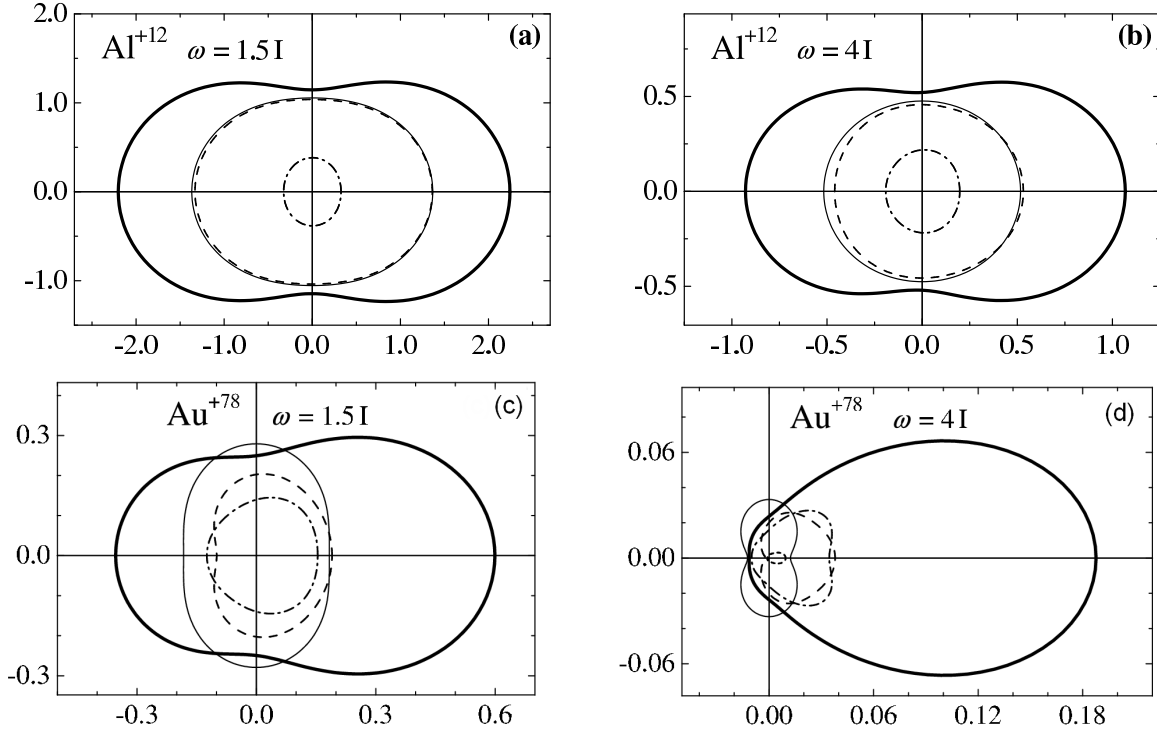


**Figure 3.** Profiles of the angular distribution of PBrS  $d^2\sigma_{\text{pol}}(\omega, \Omega)$  for collisions of 3 GeV protons with  $\text{Al}^{+12}$  (figures a and b), and  $\text{Au}^{+78}$  (c and d) ions calculated for two photon energies. In figures a and c  $\omega = 1.5I$ , in figures b and d  $\omega = 4I$ . Thick solid curves stand for the fully relativistic calculations (18), thin solid curves correspond to the non-relativistic dipole-photon approximation (19). The dashed, dotted, and dash-dotted curves correspond to the contributions of the terms proportional to the squares of the moduli of the polarizabilities  $\alpha_1(\omega, q, k)$ ,  $\beta_1^{(0)}(\omega, q, k)$  and  $\beta_1^{(1)}(\omega, q, k)$ , respectively.

formulae presented in [12, 13] one can establish, that the coefficient  $a_1(\omega)$  in (20) is proportional to the cross-terms containing the products of the relativistic polarizability  $\beta_1^{(0)}(\omega, q, k)$  of a ‘magnetic’-type with the polarizabilities  $\beta_1^{(1)}(\omega, q, k)$  and  $\alpha_1(\omega, q, k)$  which belong to the ‘electric’-type. The coefficient  $a_1(\omega)$  contains the quadratic forms of the polarizabilities of the same type, i.e. the terms proportional to  $|\beta_1^{(\lambda)}(\omega, q, k)|^2$  (with  $\lambda = 0, 1$ ) and to  $\alpha_1(\omega, q, k) \beta_1^{(1)}(\omega, q, k)$ . The magnitude of  $a_1(\omega)$  relative to  $a_2(\omega)$  is defined by the ratios  $|\beta_1^{(0)}(\omega, q, k)/\beta_1^{(1)}(\omega, q, k)|$  and  $|\beta_1^{(0)}(\omega, q, k)/\alpha_1(\omega, q, k)|$  which increase with the photon energy  $\omega$  or/and the charge of the nucleus  $Z$ , i.e. the factors responsible for the magnitude of the relativistic effects in atomic radiative processes.

The arguments presented above are illustrated by figure 3 where the profiles of  $d^2\sigma_{\text{pol}}(\omega, \Omega)$  calculated for a 3 GeV proton collision with low- $Z$  ( $\text{Al}^{+12}$ ) and high- $Z$  ( $\text{Au}^{+78}$ ) hydrogen-like ions. For each ion the calculations were performed for two photon energies equal to  $1.5I$  and  $4I$  ( $I$  stands for the ionization potential of the target). In these plots the length of the segment connecting the origin and a curve point equals the

value of  $d^2\sigma_{\text{pol}}(\omega, \Omega)$  (in millibarn/srad) in the corresponding direction. The horizontal axis ( $\theta = 0$ ) is directed along the initial momentum  $\mathbf{p}_1$ . The thick solid curve stand for a full relativistic calculation of the cross section (18). The contributions to  $d^2\sigma_{\text{pol}}(\omega, \Omega)$  from the terms proportional containing  $|\beta_l^{(0)}(\omega, q, k)|^2$ ,  $|\beta_l^{(1)}(\omega, q, k)|^2$ , and  $|\alpha_l(\omega, q, k)|^2$  is plotted are also shown in the figure. Note, that the sum of these contribution is not equal to  $d^2\sigma_{\text{pol}}(\omega, \Omega)$  which, in addition, contains the contribution of the cross-terms. The thin solid curve in each graphs represents the non-relativistic dipole-photon cross section (19).

It is seen that in contrast to the symmetric shape of  $d^2\sigma_{\text{pol}}^{\text{NR}}(\omega, \Omega)$ , the relativistic angular distribution is asymmetric, being enhanced in the forward direction. The asymmetry increases with  $\omega$  and  $Z$ .

More detailed analysis of relativistic and non-dipole effects in the spectral and spectral-angular distributions is carried out in [13].

### 3. BrS in collision of two relativistic complex particles.

In this section we outline the specific features which appear in the BrS process when both of the colliders, a projectile and a target, are complex particles (atoms, ions). It is assumed that the relative motion of the colliders occurs with relativistic velocities (in contrast to section 4 in [1] where the non-relativistic collisions were considered), whereas the internal dynamics of the colliders is described in non-relativistic terms. The theory of this process was developed in [6–8] where one can find the details of the formalism as well as the analysis of a number of physical phenomena and the limiting cases.

In what follows we mark all the quantities referring to a projectile atom (or ion) with the index ‘1’, the index ‘2’ is designated for a target atom/ion which is at rest (in the laboratory frame) before the collision.

The atomic system of units is used.

The Feynman diagrams describing the amplitude of the process are presented in figure 4. The upper double line in each diagram refers to the projectile, the lower line describes the target, the dashed line marked with  $(\omega, \mathbf{k})$  stands for the emitted photon, and the inner dashed line describes the (retarded) interaction between the colliders. The initial, intermediate and final states of each collider are characterized with the energy (this includes the rest energy, the kinetic energy and the energy due to the internal dynamics) and the momentum. The two upper diagrams describe the amplitude  $f_1$  of the photon emission by a projectile which is virtually polarized by the target, the lower pair of diagrams represents  $f_2$ , which is the amplitude of the photon emission by the target. The total BrS amplitude is given by the sum  $f_1 + f_2$ .

In contract to the non-relativistic case (see section 4 in [1] or the original papers [35, 36]), where the analytic expression for  $f_1$  can be obtained from that for  $f_2$  by exchanging the characteristics of the atoms ‘1’ and ‘2’, in the relativistic collisions one should take care on the Lorenz transformations of various quantities which constitute the amplitudes. Therefore, to construct the amplitudes it is convenient, from the very

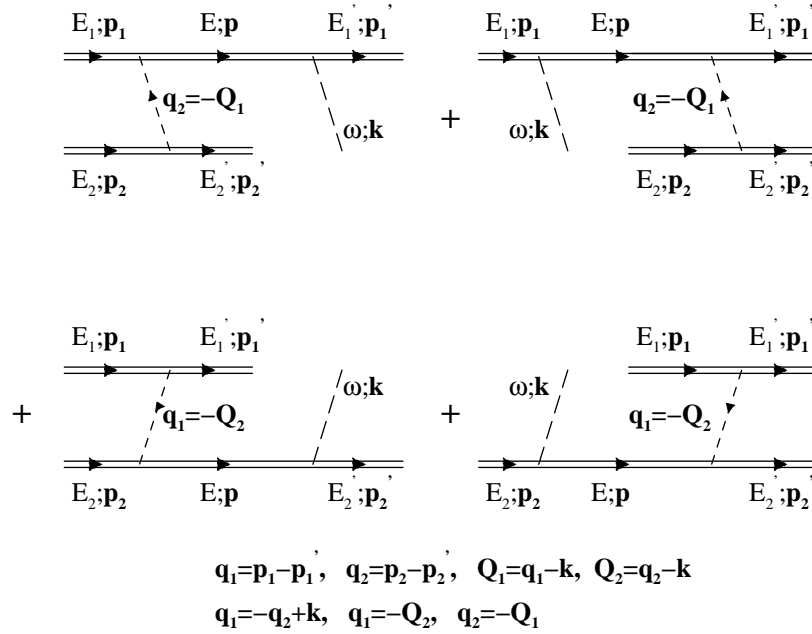


**Figure 4.** Diagrammatical representation of the BrS amplitude in relativistic atom-atom collision.

beginning, to operate with the four-vectors and four-tensors which allow one to carry out all necessary transformation of the quantities using the standard rules of quantum electrodynamics [25]. Then, the amplitudes  $f_1$  and  $f_2$  can be written in the covariant form:

$$\begin{cases} f_2 = J_\mu^{(1)}(\mathbf{q}_1) D^{\mu\nu}(E_1 - E_1', \mathbf{q}_1) T_{\lambda\nu}^{(2)}(\omega, \mathbf{k}, \mathbf{Q}_2) e^\lambda \\ f_1 = J_\mu^{(2)}(\mathbf{q}_2) D^{\mu\nu}(E_2 - E_2', \mathbf{q}_2) T_{\lambda\nu}^{(1)}(\omega, \mathbf{k}, \mathbf{Q}_1) e^\lambda. \end{cases} \quad (21)$$

Here  $e^\lambda$  is the 4-vector of the photon polarization,  $J_\mu^{(j)}(\mathbf{q}_j)$  ( $j = 1, 2$ ) is the four-current of the  $j$ th collider due to the interaction with the virtual emission,  $T_{\lambda\nu}^{(j)}(\omega, \mathbf{k}, \mathbf{Q}_j)$  is the four-tensor which describes the dynamic reaction of the particle to the action of the fields of the emitted and the virtual photons, and  $D^{\mu\nu}(E_j - E_j', \mathbf{q}_j)$  is the photon propagator. The momenta  $\mathbf{q}_j$  and  $\mathbf{Q}_j$  are explained in figure 4.

To calculate the quantities  $J_\mu^{(j)}(\mathbf{q}_j)$  and  $T_{\lambda\nu}^{(j)}(\omega, \mathbf{k}, \mathbf{Q}_j)$  one can first consider them in the rest frame of the  $j$ th collider, and then recalculate into the laboratory frame using the Lorentz transformations rules. This formalism is described in detail in [6–8], where a careful analysis of the kinematic domains, which are of the most importance for the BrS process, was carried out as well. Omitting the details of the evaluation and the analysis we present the final formulae for  $f_{1,2}$ . These look differently in the cases: (a) a collision of two neutral complexes (e.g., atom-atom), and (b) a collision involving an ionic complex (e.g., ion-atom or ion-ion). The physical nature of the differences in the formula will be given below.



In atom-atom collision the BrS amplitudes read

$$\begin{cases} f_2 = \frac{4\pi}{c} \frac{Z_1 - F^{(1)}(q_1^\perp)}{(q_1^\perp)^2} (\mathbf{e}\mathbf{q}_1^\perp) \omega \alpha^{(2)}(\omega, q_1^\perp) \\ f_1 = \frac{4\pi}{c} \frac{Z_2 - F^{(2)}(q_1^\perp)}{(q_1^\perp)^2} \left[ \tilde{\omega} \mathbf{e}\mathbf{q}_1^\perp + \gamma(\mathbf{e}\mathbf{v}_1)(\mathbf{k}\mathbf{q}_1^\perp) \right] \alpha^{(1)}(\tilde{\omega}, q_1^\perp), \end{cases} \quad (22)$$

The ion-atom/ion collision is described by

$$\begin{cases} f_2 = \frac{4\pi}{c} \frac{Z_1}{q_1^2 - \omega^2/c^2} \left[ \mathbf{e}\mathbf{q}_1 - \frac{\omega}{c^2} \mathbf{e}\mathbf{v}_1 \right] \omega \alpha_d^{(2)}(\omega), \\ f_1 = \frac{4\pi}{c} \frac{Z_2}{q_2^2} \left[ \tilde{\omega} \mathbf{e}\mathbf{q}_2^\perp + \gamma(\mathbf{e}\mathbf{v}_1)(\mathbf{k}\mathbf{q}_2^\perp) - \frac{\tilde{\omega}}{\gamma^2} \mathbf{e}\mathbf{q}_1^\parallel \right] \alpha_d^{(1)}(\tilde{\omega}). \end{cases} \quad (23)$$

In these formulae  $\mathbf{q}_j^\perp$  and  $\mathbf{q}_j^\parallel$  stand for the perpendicular (' $\perp$ ') and the parallel (' $\parallel$ ') components of  $\mathbf{q}_j$  with respect to the initial velocity  $\mathbf{v}_1$  of the projectile,  $\gamma = (1 - v_1^2/c^2)^{1/2}$  is the relativistic Lorentz factor. The quantity  $\omega$  is the photon energy measured in the laboratory frame (the rest frame of the target). The photon emitted by the projectile and measured in its rest frame also has energy  $\omega$ , however, due to the Doppler effect, in the laboratory frame this energy is changed according to the rule  $\omega \rightarrow \tilde{\omega} = \gamma\omega(1 - \beta \cos \theta)$ , where  $\beta = v_1/c$  and  $\theta$  is the emission angle in the laboratory frame. The notations  $Z_j$  stand for the charges of the nucleus,  $Z_j$  (in (23)) are the net ionic charges,  $F^{(j)}(q)$  denote the form-factors. The functions  $\alpha^{(j)}(\omega, q)$  are non-relativistic generalized dynamic dipole polarizabilities of the colliders,  $\alpha_d^{(1)}(\omega)$  are dynamic dipole polarizabilities.

The amplitude  $f_2$  from (22) coincides with its non-relativistic analogue (see [1], first term in Eq. (31)). This coincidence has a clear physical explanation. The BrS process in the collision of two neutral atoms occurs, mainly, when the distance between the two nuclei is less than the radius of each atom,  $r \leq R_{\text{at}}$ . At such distances the effect of retardation is small. Additionally, it can be shown [6, 7] that in such collisions the parallel component of the transferred momentum is small, so that  $\mathbf{q} \approx \mathbf{q}_1^\perp$ .

The component  $\mathbf{q}_1^\perp$  is not affected by the Lorentz transformation with respect to the velocity  $\mathbf{v}_1$ . Therefore, as it is seen from (22), the amplitude  $f_1$  can be obtained from  $f_2$  by choosing the frame moving with the velocity  $\mathbf{v}_1$  (instead of the laboratory frame) and, then, exchanging the colliders indices.

The BrS process in ion-ion (or ion-atom) collisions is governed by another regime [8]. In this case, due to the presence of the non-zero net charges, the colliders can be effectively polarized even being separated by a large distance,  $r \gg R_{\text{at}}$ . Therefore, the retardation becomes very important. This explains the factor  $q_1^2 - \omega^2/c^2$  in the denominator in the first expression from (23). The dominating role of large distances is also reflected by the fact that the amplitudes  $f_1$  and  $f_2$  are expressed in terms of the polarizabilities  $\alpha_d^{(1)}(\tilde{\omega})$  and  $\alpha_d^{(2)}(\omega)$  rather than via the generalized polarizabilities as in (22). Additionally, in contrast to the neutral atoms collision, both components, the transverse and the parallel, of the vectors  $\mathbf{q}_j$  are important in ionic collisions, which explains the additional terms in square brackets in (23).

Formulae (22) and (23) allow one to analyze the spectral and spectral-angular dependence of BrS formed in collision of relativistic complex particles [6–8]. These dependences include the contributions of the radiation by the target, the projectile and the interference term. Not going to reproduce rather long expressions we mention the most important features of these distributions.

For all types of the collision the leading terms in the angular distribution of the dipole PBrS emitted by the target and the projectile can be presented in the following general forms:

$$\begin{cases} \frac{d^2\sigma_2}{d\omega d\Omega} = C_2 (1 + \cos^2 \theta) \\ \frac{d^2\sigma_1}{d\omega d\Omega} = C_1 (1 + \cos^2 \tilde{\theta}) \left(\frac{\tilde{\omega}}{\omega}\right)^2, \end{cases} \quad (24)$$

where the coefficients  $C_{1,2}$  are independent on the emission angle  $\theta$ . Omitting details we mention that for atom-atom collisions these coefficients weakly depend on the projectile energy, whereas in the ion-ion/atom case they logarithmically increase with  $\gamma = E/M_1 c^2$ . This happens due to the same reasons which are mentioned above in connection with the PBrS of a structureless particle (see (14), (16) and figure 2).

It is seen from (24), that the radiation by the target,  $d^2\sigma_2/d\omega d\Omega$ , is proportional to  $(1 + \cos^2 \theta)$ , i.e. is distributed as that emitted by a rotating dipole [3]. This is a common feature and it does not depend either on the type of the projectile (light, heavy, structureless or complex) nor on the type of the interaction between the colliders. Apart from the collisions of the atomic particles this dipole-type profile of the angular distribution was found in a neutron and a neutrino BrS process in collisions with atoms [37, 38], and in nuclear collisions [39, 40]. Beyond the non-relativistic dipole approximation and in the case when the internal dynamics of the target must be treated relativistically, the profile of the angular distribution strongly deviates from the  $(1 + \cos^2 \theta)$  law (see figures 3c,d).

The PBrS of the projectile,  $d^2\sigma_1/d\omega d\Omega$ , has another angular dependence. As mentioned above, the photon energy emitted by the projectile is Doppler-shifted,  $\omega \rightarrow \tilde{\omega}$ . This results in the factor  $(\tilde{\omega}/\omega)^2 \propto (1 - \beta \cos \theta)^2$  which strongly deviates from one in the case of high velocities, when  $\beta = v_1/c \sim 1$ . Additional modification of the angular dependence is due to the aberration effect. The quantity  $\tilde{\theta}$ , on the right-hand side of the second equation from (24), stands for the emission angle in the rest frame of the projectile. In the laboratory frame this angle is becomes aberrated and is related to  $\theta$  via  $\cos \tilde{\theta} = (\cos \theta - \beta)/(1 - \beta \cos \theta)$  [3]. Therefore, the profile of  $d^2\sigma_1/d\omega d\Omega$  is defined by  $\mathcal{P}(\theta, \beta) \equiv (1 + \beta^2)(1 + \cos^2 \theta) - 4\beta \cos \theta$ . This function explicitly demonstrates a remarkable feature of the PBrS by a relativistic complex projectile. Namely, it does not contain the well-known peculiarity typical for the ordinary BrS, where the radiation is concentrated in a narrow cone  $\theta \leq \gamma^{-1}$  in the forward direction. Indeed, the function  $\mathcal{P}(\theta, \beta)$  exhibit an opposite property: the radiation emitted in the forward direction,  $\theta = 0$ , is less intensive than in the backward direction,  $\theta = \pi$ . In the non-relativistic limit the function  $\mathcal{P}(\theta, \beta)$  reduces to the dipole-type profile  $\mathcal{P}(\theta, 0) = (1 + \cos^2 \theta)$  [36].

On the basis of the detailed analysis carried in [7, 8] the following criterion was formulated on the magnitude of the ratio  $\xi = (d^2\sigma_1/d\omega d\Omega)/(d^2\sigma_2/d\omega d\Omega)$  in different ranges of  $\omega$  and  $\theta$ . It was shown, that if the photon energy and the emission angle are chosen to satisfy the inequality  $(\tilde{\omega}/c)^2 |\alpha^{(1)}(\tilde{\omega}, q_1^\perp)|^2 \gg |\alpha^{(2)}(\omega, q_1^\perp)|^2$ , then the PBrS of the projectile dominates in the total spectrum over the radiation emitted by the target. In the inequality sign is opposite then the target radiates more intensively. Therefore, for sufficiently high velocities of the collision there is a possibility to separate the radiation by the two colliders.

Another important feature of the BrS process at relativistic velocities, which is due to the Doppler and the aberration effects, is that the intensity of the dipole radiation formed in symmetric collisions does not vanish. Indeed, if one considers two identical colliders then the total amplitude of the BrS  $f_1 + f_2 \neq 0$  (see (23)). We note that in the non-relativistic symmetric collision the emission of the dipole photon is strictly forbidden and  $f_1 + f_2 = 0$  (see section 4 in [1] or the original papers [35, 36]).

#### 4. Conclusions.

In this paper reviewed the progress which have been achieved in theoretical description of the PBrS process with account for the relativistic effects. We concentrated mainly on the polarizational part of the total BrS spectrum. This mechanism defines the emission spectrum formed in collisions of heavy projectiles with many-electron targets. In the case of a structureless heavy projectile the main characteristics of the spectrum can be accurately computed using the algorithms which have been developed recently on the basis of the formalism described in section 2. The main difficulty, on the numerical level, is in the accurate and efficient calculation of the relativistic generalized polarizabilities of a many-electron target. Compared to the non-relativistic case this is a more complicated problem, and at present we cannot state that these quantities can be efficiently computed in arbitrary ranges of the photon energies, transferred momentum and the multipolarity index. However, the calculations which have been already performed indicated that the relativistic effects of all types, – i.e. those related to the motion of the colliders, including the internal dynamics, the effect of retardation and the radiation in multipoles, must be accounted for in order to obtain reliable results.

Note that if a relativistic projectile has the internal structure of a relativistic nature, it is not necessary to develop a new formalism describing the PBrS emitted by the projectile. Instead, the corresponding formulae can be obtained from those presented 2 using the Doppler and the aberration of light transformation as it is described in 3. With slight modifications the formalism discussed above can be applied for other colliding systems, where relativistic effects are important. Calculations for relativistic heavy-ion collisions are of interest because of recent experimental efforts in this direction [41]. For example, one can describe the BrS arising in relativistic collisions involving nuclei. In this case the dynamic polarization of the colliders results in the photon emission via the PBrS mechanism, and the main contribution comes from the non-dipole radiation

(quadrupole and higher).

For a light projectile, an electron or a positron, the total BrS problem cannot be considered in terms of the polarization mechanism only. The full theory must include, from the very beginning, the two terms in the amplitude,  $f_{\text{ord}}$  and  $f_{\text{tot}}$ . As a result, the total BrS cross section  $d\sigma_{\text{tot}}$  includes the ordinary  $d\sigma_{\text{ord}}$  and the polarizational  $d\sigma_{\text{pol}}$  parts, which are positive, and the interference term  $d\sigma_{\text{int}}$  which can be of either sign. In the non-relativistic domain and within the dipole-photon scheme the features of  $d\sigma_{\text{tot}}$  are known quite well (see, e.g. ([1])). From the formal viewpoint the theory of the BrS process of a light projectile, which incorporates all relativistic effects, has been developed. Indeed, the formalism for the PBrS presented in [12, 13] and sketched above in section 2 combined with that for the ordinary BrS [26] (see also [42] where the relativistic DPWA is compared with simpler theories) allows one, in principle, to obtain the characteristics of the total BrS. The calculation, within fully relativistic scheme, of the cross section  $d\sigma_{\text{pol}}$  of an electron now can be implemented. For example, the data presented in section 2 for a 3 GeV positron can be also attributed for an electron of the energy  $\varepsilon_1 \approx 1.5$  MeV, since the PBrS part of the spectrum is nearly independent on the mass of a projectile. Thus, one can estimate the total cross section as a sum of the two terms  $d\sigma_{\text{tot}} \approx d\sigma_{\text{ord}} + d\sigma_{\text{pol}}$  where  $d\sigma_{\text{ord}}$  can be taken from the tables [43, 44]. This approach completely ignores the interference term  $d\sigma_{\text{int}}$ . The calculation of the total BrS cross section based on the approximation  $d\sigma_{\text{tot}} \approx d\sigma_{\text{ord}} + d\sigma_{\text{pol}}$  were carried out recently in [10]. This was done within the ‘logarithmic approximation’ and for the dipole-photon radiation only. The relativistic effects due to the internal dynamics of the target electrons were not accounted for as well. However, it is not at all evident that the term  $d\sigma_{\text{int}}$  can be ignored on the basis of simple approaches. As figures 3 demonstrate, the relativistic effects noticeably modify the angular distribution of PBrS leading to the increase of the emission in the forward direction. Since the OBrS of a relativistic projectile is also emitted mostly in the forward direction the interference of the two mechanisms can be important. The approach which allows one to account for the interference was proposed in [9], where analytic expressions and the numerical results for the total BrS spectra from neutral atoms and ions were presented for electron scattering at energies 10 – 2000 keV. In the cited paper the ‘stripping approximation’, derived initially [23, 24] for a non-relativistic electron–atom scattering, was extended to the case of the relativistic velocities of the collision. On the basis of this model approach (which does not accurately account for the retardation effects and for the multipole character of the radiation) the analysis of the modification of the BrS spectrum due to the influence of the PBrS channel was carried out.

At present, there are no accurate numerical results on the total BrS spectra and angular distributions of relativistic electrons/positron on many-electron targets which account for all important relativistic effects and for the two mechanisms of the photon emission. Let us stress that such calculations will be an important step forward towards precise comparison with the recent experimental data on the BrS obtained for collisions of 10 – 100 keV electrons with various targets [45]. The mostly recent experiments [46],

where for the first time the measurement of the absolute values of the BrS cross section in electron scattering from noble gas atoms were reported, show some indications on the significance of the PBrS in the energy ranges in which the relativistic treatment of the process is necessary.

## Acknowledgments

This work is supported by the Russian Foundation for Basic Research (Grant No 96-02-17922-a) and INTAS (Grant No 03-51-6170). AVK acknowledges the support from the Alexander von Humboldt Foundation.

## References

- [1] Korol, A. V., Solov'yov, A. V., 2005. Radiat. Phys. Chem. this issue.
- [2] Akhiezer, A. I., Berestetskii V. B., 1969. Quantum Electrodynamics. Nauka, Moscow.
- [3] Landau, L. D., Lifshitz, E. M., 1975. The Classical Theory of Fields. Pergamon, Oxford.
- [4] Amusia, M. Ya., Kuchiev, M. Yu., Korol, A. V., Solov'yov, A. V., 1985. Sov. Phys. - JETP 61, 224-228.
- [5] Astapenko, V. A., Buimistrov, V. M., Krotov, Yu. A., Mihailov, L. K., Trakhtenberg, L. I., 1985. Sov. Phys. - JETP 61, 930.
- [6] Amusia, M. Ya., Kuchiev, M. Yu., Solov'yov, A. V., 1987. Sov. Phys. - Tech. Phys. 32, 499-500.
- [7] Amusia, M. Ya., Kuchiev, M. Yu., Solov'yov, A. V., 1988. Sov. Phys. - JETP 67, p.41-48.
- [8] Amusia, M. Ya., Solov'yov, A. V., 1990. Sov. Phys. - JETP 70, 416-425.
- [9] Avdonina, N. B., Pratt, R. H., 1999. J. Phys. B 32, 4261-4276.
- [10] Astapenko, V. A., Bureeva, L. A., Lisitsa, V. S., 2000. JETP 90, 788-794.
- [11] Korol, A. V., Lyalin, A. G., Obolenski, O. I., Solov'yov, A. V., Solovjev, I. A., 2001. In: Dugganm J. L., Morgan, I. L. (Eds.) AIP Conference Proceedings, vol. 576. AIP Press, pp. 64-67.
- [12] Korol, A. V., Obolenskiy, O. I., Solov'yov, A. V., Solovjev, I. A., 2001. J. Phys. B 34, 1589-1617.
- [13] Korol, A. V., Lyalin, A. G., Obolenskiy, O. I., Solov'yov, A. V., Solovjev, I. A., 2002. JETP 94, 704-719.
- [14] Korol, A. V., Obolenskiy, O. I., Solov'yov, A. V., Solovjev, I. A., 2002. Surface Review and Letters 9, 1191-1195.
- [15] Blazhevich, S.V., Cherpunov, A.S., Grishin, V.K., et. al., 1996. Phys. Lett. A 211, 309-312.
- [16] Nasonov, N. N., 1998. Nucl. Instrum. Methods B 1998 145, 19-24.
- [17] Blazhevich, S.V., Cherpunov, A.S., Grishin, V.K., et. al., 1999. Phys. Lett. A 254, 230-232.
- [18] Kamyshanchenko, N., Nasonov, N., Pokhil, G., 2001. Nucl. Instrum. Methods B 173, 195-202.
- [19] Astapenko, V. A., Buimistrov, V. M., Krotov, Yu. A., Nasonov, N. N., 2004. Phys. Lett. A 332, 298-302.
- [20] Astapenko, V. A., Bureeva, L. A., Lisitsa, V. S., 2002. Phys. Usp. 45, 149-184.
- [21] Zon, B. A., 1977. Sov. Phys. - JETP 46, 65.
- [22] Amusia M. Ya., Zimkina T. M., Kuchiev M. Yu., 1982. Sov. Phys. - Tech. Phys. 27, 866.
- [23] Amusia, M. Ya., Avdonina, N. B., Chernysheva, L. V., Kuchiev, M. Yu., 1985. J. Phys. B 18, L791-L796.
- [24] Buimistrov, V.M., Trakhtenberg, L. I., 1977. Sov. Phys. - JETP 46, 447.
- [25] Berestetskii, V. B., Lifshitz, E. M., Pitaevskii, L.P., 1982. Quantum Electrodynamics. Pergamon, Oxford.
- [26] Tseng, H. K., Pratt, R. H., 1970. Phys. Rev. A 3 100-115.
- [27] Tseng, H. K., 1997. J. Phys. B 30, L317-L321. (Corrigendum: 2000. ibid. 33, 1471.)
- [28] Korol, A. V., 1992. J. Phys. B 25, L341-L344.

- [29] Korol, A. V., Lyalin, A. G., Solovyov, A. V., Avdonina, N. B., Pratt, R. H., 2002. *J. Phys. B* 35, 1197-1210.
- [30] Varshalovich, D. A., Moskalev, A. N., Khersonskii, V. K., 1988. *Quantum Theory of Angular Momentum*. World Scientific, Singapore.
- [31] Lindgren, I., Morrison, J., 1986. *Atomic Many-Body Theory*. Springer, Berlin.
- [32] Chernysheva, L. V., Yakhontov, V. L., 1999. *Comp. Phys. Comm.* 119, 232-249.
- [33] Amusia, M. Ya., Korol A. V., 1992. *J. Phys. B* 25, 2383-2392.
- [34] Amusia, M. Ya., Avdonina, N. B., Kuchiev, M. Yu., Chernysheva, L. V., 1986. *Izv. Acad. Nauk SSSR: Ser. Fiz.* 50, 1261-1266.
- [35] Amusia, M. Ya., Kuchiev, M. Yu., Solov'yov, A. V., 1984. *Sov. Phys. - Tech. Phys. Lett.* 10, 431-432.
- [36] Amusia, M. Ya., Kuchiev, M. Yu., Solov'yov, A. V., 1985. *Sov. Phys. - JETP* 62, 876-881.
- [37] Amusia, M. Ya., Baltenkov, A. S., Zhalov, M. B., Korol, A. V., Solov'yov, A. V., 1986. *Polarizational bremsstrahlung in scattering of particles at atoms and nuclei.- Proceedings of 21st Winter School of Leningrad Institute of Nuclear Physics*, pp.135-194 (in Russian).
- [38] Amusia, M. Ya., Baltenkov, A. S., Korol, A. V., Solov'yov, A. V., 1987. *Sov. Phys. - JETP* 66, 877-883.
- [39] Hubbard, D. F., Rose, M. E., 1966. *Nucl. Phys.* 84, 337.
- [40] Amusia, M. Ya., Solov'yov, A. V., 1987. In: Sushkov, O. P. (ed.), *Modern Developments in Nuclear Physics*, World Scientific, Singapore, pp. 425-437.
- [41] Ludziejewski, T., Stöhlker, T., Keller, S., et. al., 1998. *J. Phys. B* 31, 2601-2609.
- [42] Shaffer, C. D., Pratt, R. H., 1997. *Phys. Rev. A* 56, 3653-3658.
- [43] Pratt, R. H., Tseng, H. K., Lee, C. M., Kissel, L., MacCallum, C., Riley, M., 1977. *At Data Nucl. Data Tables* 20, 175-209 (Erratum: 1981. *ibid.* 26, 477-481).
- [44] Kissel, L., Quarles, C. A., Pratt, R. H., 1983. *At. Data Nucl. Data Tables* 28, 381.
- [45] Quarles, C. A., Portillo, S., 1999. In: Duggan J. L., Morgan, I. L. (Eds.) *AIP Conference Proceedings*, vol. 576. AIP Press, pp. 174-177.
- [46] Portillo, S., C. A. Quarles, C. A., 2003. *Phys. Rev. Lett.* 91, 173201.